Garozzo, D., *et al.*: Comparison of the Reactive Control Strategies in …
THERMAAL SCIENCE: Year 2018, Vol. 22, Suppl. 3, pp. S887-S896

S887

COMPARISON OF THE REACTIVE CONTROL STRATEGIES IN LOW VOLTAGE NETWORK WITH PHOTOVOLTAIC GENERATION AND STORAGE

by

Dario GAROZZO[a], Giuseppe Marco TINA[a], and Dezso SERA[b]*

[a] DIEEI, University of Catania, Catania, Italy
[b] Aalborg University, Aalborg, Denmark

The aim of this study is to analyze the different decentralized voltage control strategies, based on the reactive power control of photovoltaic inverters. The study focuses on evaluating their impact in terms of reactive power demanded from the grid, due to the regulation, and active losses in the network and in the photovoltaic inverters. In a second step, the presence of battery energy storage systems in the network is considered and further analysis are performed, in order to take into account the overvoltage mitigation by peak shaving of the photovoltaic generation. All the simulations are performed in MATLAB/SIMULINK, where the model of a single-phase low-voltage distribution network with distributed generation sources is implemented.

Key words: inverter losses, photovoltaic inverters, radial network, reactive power control, storage systems, voltage regulation

Introduction

In recent years, power systems have seen a drastic change, with the continuous growth of the renewable energy sources, especially in the number of photovoltaic (PV) installation. In 2015, the world installed capacity of PV systems amounted to 51 GW [1]. Thanks to this yearly development, the global installed PV power in the world is up more than 227 GW. In 2014, the total PV energy production in Italy reached the value of 22306 GWh [2]. With the rapidly increasing penetration of these distributed generation systems, their effect on the grid is in terms of stability and power quality is also increasing. Therefore, the challenge is the development of a smart grid, able to manage the increasing penetration of the distributed generation [3]. The highest penetration of PV systems is at the distribution level, in fact 95% of the PV systems are connected to the medium voltage (MV) and low voltage (LV) level [4], in which the topology of the network is essentially radial. At micro-generating level, the European Standard CENELEC EN 50438 contains the rules for the connection of electrical power plants with a rated current below 16 A, to the LV distribution network [5, 6]. For what concerns the voltage quality, the European Standard EN 50160 limits the voltage deviation to an interval of ±10% of the rated value [7]. Large PV power plants are already required by many grid operators to be able to provide grid support functionalities, such as frequency sen-

_____

* Corresponding author, email: giuseppe.tina@dieei.unict.it

S888

Garozzo, D., *et al.*: Comparison of the Reactive Control Strategies in …
THERMAL SCIENCE: Year 2018, Vol. 22, Suppl. 3, pp. S887-S896

sitive mode, fault ride through, and voltage support [8]. Reactive power based voltage support strategies are seen as a viable medium term solution for increasing the penetration of PV without violating voltage deviation limits set by the standards [9]. In presence of grid connected PV systems, different voltage regulation strategies, based on the reactive power control of the PV inverters can be adopted. Each of them could have a different impact on the network, in terms of reactive power exchanges and active power losses in the network and in the inverters, due to the reactive power control [10].

However, reactive power based voltage support strategies have their limitations in preventing overvoltage, especially in networks with low X/R ratio, typically the case for LV distribution network (LVDN). In these networks, higher reactive power needs to be absorbed (*i. e.* lower power factor) for the same voltage reduction effect, hence increasing line and inverter losses and risking overloading both lines and distribution transformers.

In LVDN with R being high, and from the expression of industrial voltage drop, it is foreseen that active power has a great effect on voltage, so energy storage can be an effective solution for preventing overvoltage due to high PV production, since excess power can be used to charge the batteries while the power injected to the grid can be limited to safe level. The stored energy can then be fed to the grid or consumed locally when solar production is low. While home battery energy storage is becoming increasingly popular, their penetration is still relatively low in most networks. In those cases, battery energy storage systems (BESS) alone may not be able to effectively eliminate the overvoltage during high PV production.

Therefore, the aim of this paper is to evaluate the effect of the installation of the storage on the mitigation of overvoltage problems in a LV network, by combining various reactive power based voltage support strategies with various amounts of BESS in the network.

Power system description and model

A typical topology of a LV radial distribution network is considered in this study, fig. 1. Node 1 represents the MV busbar, *i. e.* the connection point between the LV network and the higher voltage level grid. All nodes from 2 to 10 hold a 5 kWp PV system and a typi-
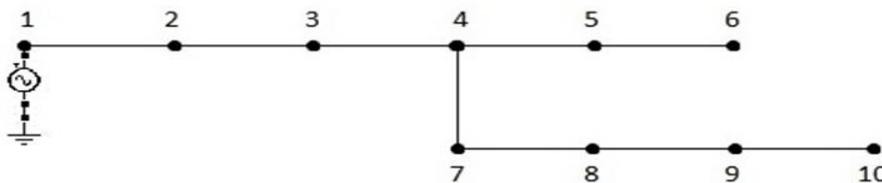

Figure 1. Topology of the radial LV network

cal residential load (3 kWp), modeled as a constant PQ load, in which the active power demand is constant for an hour. For the active power curve, a typical daily profile is adopted. In a second step also the installation of a storage system in the nodes will be considered. Concerning Q, even if the $\cos\varphi$ of the load could change between 0.7 and 0.9 during the day, a load with a $\cos\varphi = 0.9$ is adopted, since it represents the worst case for the overvoltage problem, as discussed in [11]. The PV output is obtained from a daily simulation, in which typical trends of global irradiance and daily ambient temperature are used as inputs. Historical data are used for this scope, considering the values of irradiance and temperature of a typical day of June in Sicily. The lines are modeled using the RL equivalent circuits, with a resistance, $r = 0.576$ Ω/km, and a longitudinal reactance, $x = 0.397$ Ω/km, except for the line 1-2, in which $RT = 0.0253$ Ω and $XT = 0.025$ Ω, since they represent typical values of the line parameters.

In order to investigate the impact of the storage and its dynamic behavior, the two time-constants model of a Li-ion battery was implemented in MATLAB/SIMULINK [12]. The state of charge (SOC) is estimated by the Coulomb counting method. For the model parameters EO_C (SOC), R_i (SOC), R_1 (SOC), C_1 (SOC), R_2 (SOC), C_2 (SOC), the values proposed in [13] are used. Since the model is not very accurate for low levels and high level of the SOC, a depth of discharge (DOD) equal to 70% and a maximum SOC of 95% are used as constrains for the battery management system (BMS).

The DC-AC converter model needs to take into account the active losses, therefore two resistors R_s (Input series resistance) and R_p (Output shunt resistance) are added to the ideal model of the inverter, implemented in [14], in order to simply evaluate the losses due to the voltage regulation, since they also depend on the reactive power absorbed by the inverter, as explained in [10] and [15]. Figure 2 shows the non-ideal inverter model used in this study. This simple model is validated with experimental data in [16], where the relationship between inverter efficiency, η_{inv}, and apparent power, S, is studied and the following formula is obtained:

$$\eta_{inv} = \frac{2R_s Sa}{V_{DC}^2 \left[1 - \sqrt{1 - 4\frac{R_s}{V_{DC}^2}\left(S + \frac{V_{AC}^2}{R_p}\right)} \right]} \tag{1}$$

where a is a parameter that can be considered equal to one, except for very low value of the power factor. The values of the two resistances for a 5 kWp PV inverter are listed in tab. 1.

This simple model allows evaluating the impact of the reactive power based voltage control on the active losses of the PV inverters, estimating the losses of the inverter without an excessive computational time.
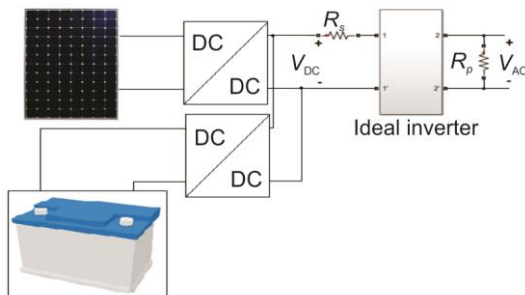
Figure 2. Model of the generic node with a non-ideal DC-AC converter

Table 1. Values of R_s and R_p for a 5 kWp PV inverter

R_s	0.8 Ω
R_p	4100 Ω

According to [17], inverter power losses can be evaluated as a function of the apparent power. They can be approximated by a second-order polynomial function, shown in fig. 3.

Each static converter must work inside its capability curve, designed starting from voltage limitation, current limitation, active power limitation and thermal limitations, related to the maximum admissible temperature, as exposed in [18]. The value $PF = 0.9$ represents the limit of this kind of constrain for all the PV inverters.

Impact of the storage on over voltages

First, the aim is to evaluate the contribution of the BESS installation in the LV network for the overvoltage correction without reactive power control. In this step, four different scenarios are considered according to the different presence of storage systems in the network: no BESS (Scenario 1), 1 BESS (Scenario 2), 4 BESS (Scenario 3), and 9 BESS (Sce-

S890

Garozzo, D., *et al.*: Comparison of the Reactive Control Strategies in …
THERMAL SCIENCE: Year 2018, Vol. 22, Suppl. 3, pp. S887-S896

nario 4). Typical BESS are considered, with a rated capacity of 80 Ah, a DOD of 70% and the charge/discharge profile shown in fig. 4.
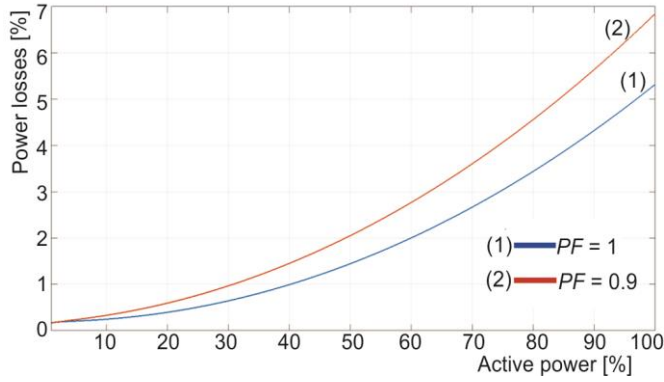

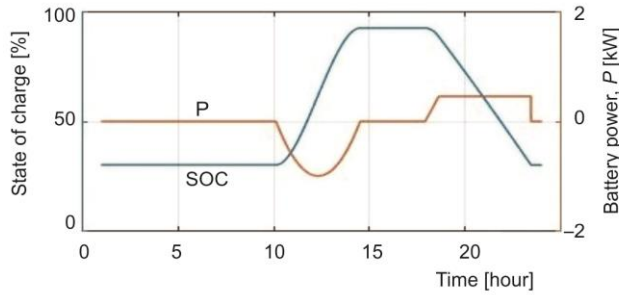**Figure 3. Inverter losses at different power factor**

Figure 4. The SOC and battery active power

Since the objective of the installation of the storage is to mitigate the overvoltage by the absorption of active power, each BESS absorbs active power during the peak hours of the PV output and it injects active power into the network during the evening. All the BESS follow the same charge/discharge curve.

For the calculation of the load flow in radial networks, a simple algorithm based on the vector analysis of voltage and current is proposed in [19]. The ab-system is defined with respect to the node 1, *i. e.* the MV/LV bus. The dq-system is defined with respect to the voltage vector at the specific node. Therefore, the vector of the voltage in each node has the direction of d-axis. In order to take into account the possibility to have a radial network with more than on branch, the algorithm can be modified:

$$\theta_n = \tan^{-1}\left(\frac{V_{a,n}}{V_{b,n}}\right) \tag{2}$$

$$I_{d,n} = \frac{P_n}{V_n} \tag{3a}$$

$$I_{q,n} = \frac{Q_n}{V_n} \tag{3b}$$

$$\begin{bmatrix} I_{a,n} \\ I_{b,n} \end{bmatrix} = \begin{bmatrix} \cos\theta_n & \sin\theta_n \\ \sin\theta_n & -\cos\theta_n \end{bmatrix} \begin{bmatrix} I_{d,n} \\ I_{q,n} \end{bmatrix} \tag{4}$$

$$I_{a,k} = \sum_{j\in\Psi} I_{a,j} \tag{5a}$$

$$I_{b,k} = \sum_{j\in\Psi} I_{b,j} \tag{5b}$$

$$V_{a,n} = V_{a,m} - R_k I_{a,k} + X_k I_{b,k} \tag{6a}$$

$$V_{b,n} = V_{b,m} - R_k I_{b,k} - X_k I_{a,k} \tag{6b}$$

Garozzo, D., *et al.*: Comparison of the Reactive Control Strategies in …
THERMAAL SCIENCE: Year 2018, Vol. 22, Suppl. 3, pp. S887-S896

S891

$$V_n = \left(V_{a,n}^2 + V_{b,n}^2 \right)^{1/2}$$ (7)

In particular, eqs. (5a) and (5b) represent the two components of the current in line k in ab-axis, where Ψ is the set of connection lines which contributes to the amount of current that flows through line k. The two components of the voltage at node n are computed in eqs. (6a) and (6b), where *n* and *m* are the nodes at the ends of the generic line k, fig. 5. The starting point of the algorithm is $V_{a,n}$ = 230 V and $V_{b,n}$ = 0 V. This generic mathematical formulation can be used also in network with a certain number of branches.

A 24-hours simulation is run and the results, in terms of voltage p.u. at all nodes, shown in the following section. In Scenario 1, fig. 6, it is noticeable that an over-voltage problem has occurred at the last nodes, in particular at nodes 8, node 9 and node 10, as expected. The worst case is for node 10, in which the overvoltage occurs from 9:00 to 14:00.
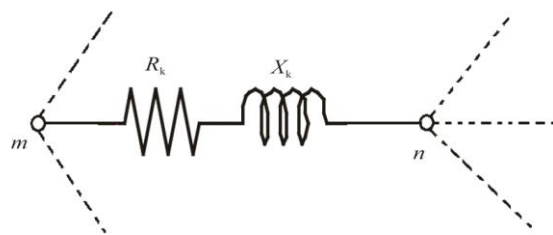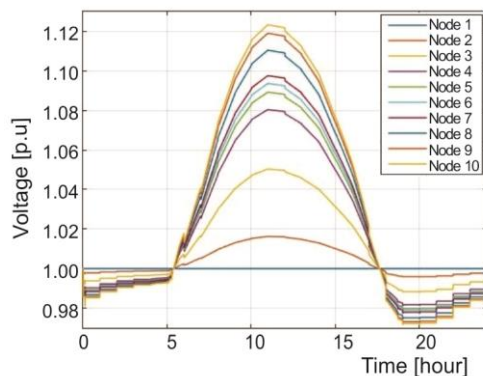
Figure 5. Generic line k

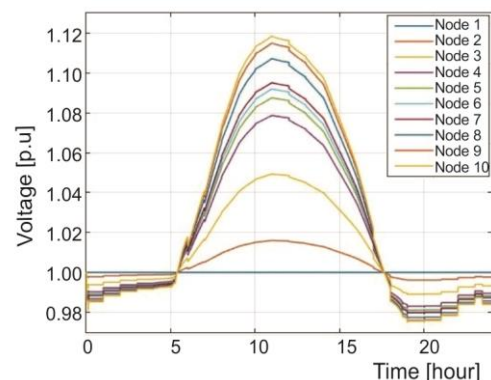**Figure 6. Voltage p.u. at all nodes in Scenario 1: no BESS** (*for color image see journal web site*)

Figure 7. Voltage p.u. at all nodes in Scenario 2: 1 BESS (*for color image see journal web site*)

In Scenario 2, fig. 7, a BESS is installed at node 10, since it represents the best choice from an overvoltage prevention point of view. The effect is a small reduction of the peak values of the voltage p.u., even if the overvoltage problem is not avoided.

In Scenario 3, fig. 8, four BESS are installed at node 3, node 6, node 7, and node 10, respectively, in order to consider a generic distribution of the storage in the network. In this case, the overvoltage problem is strongly reduced at node 8, in which it occurs for a small time interval. The peak values of the nodal voltages are also mitigated.

Finally, in Scenario 4, fig. 9, all nodes hold a storage system. This investment elimi-nates the overvoltage problem at node 8, considering a limit of 1.1 p.u., and it reduces its occurrence at the last two nodes. In particular, at node 9, the problem now occurs for a small time interval. The peak values of the voltage at the last three nodes are exposed in tab. 2. As seen, a reduction of the peak value of the voltage is observed in the scenarios with a high number of storage installations.
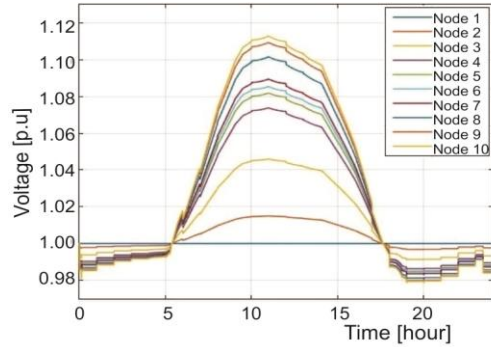
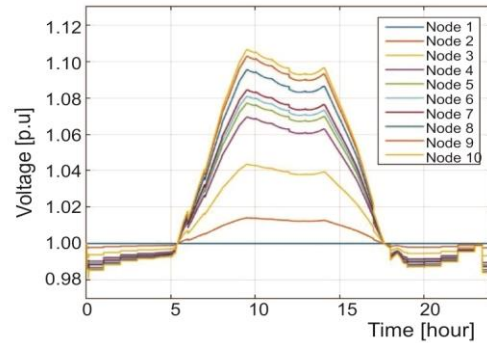**Figure 8. Voltage p.u. at all nodes in Scenario 3: 4 BESS** (*for color image see journal web site*)

Figure 9. Voltage p.u. at all nodes in Scenario 4: 9 BESS (*for color image see journal web site*)

Table 2. Maximum voltage at the critical nodes in the four scenarios

	Node 8	Node 9	Node 10
Scenario 1	255.43 V	257.41 V	258.40 V
Scenario 2	254.68 V	256.47 V	257.27 V
Scenario 3	253.38 V	255.18 V	255.98 V
Scenario 4	251.96 V	253.67 V	254.52 V

The cost of this kind of voltage control based on the active power absorbed by the storage during its charge, is related to a fixed cost due to the installation cost, a maintenance cost and the cost of power losses. In this study the battery losses are taken into account, evaluating the battery efficiency in terms of energy. For the adopted charge/discharge profile, the evaluated battery efficiency, η_{BESS}, is evaluated:

$$\eta_{BESS} = \frac{E_{out}}{E_{in}} = 0.81 \tag{8}$$

where E_{out} is the energy provided by the battery during the discharge time and E_{in} is the energy absorbed by the battery during the charge time.

Voltage control strategies and their performance

In this Section, the performances of the different voltage control strategies based on the reactive power control are evaluated for comparison purposes. Therefore, three indices of performance need to be defined. In [20], the first two parameters *QDI* and *PLI* are defined:

A)   Reactive Power Demand Index:

$$QDI\% = \frac{Qdem_{reg} - Qdem_{unreg}}{Qdem_{unreg}} 100 \tag{9}$$

B)   Network Power Losses Index:

$$PLI\% = \frac{Ploss_{reg} - Ploss_{unreg}}{Ploss_{unreg}} 100 \tag{10}$$

Garozzo, D., *et al.*: Comparison of the Reactive Control Strategies in …
THERMAAL SCIENCE: Year 2018, Vol. 22, Suppl. 3, pp. S887-S896

S893

The *QDI* defines the amount of reactive power required from the external grid, due to the voltage control, $Qdem_{reg}$, as a percentage of the reactive power demand in the case of no voltage regulation and no storage (base case), $Qdem_{unreg}$. The *PLI* defines the amount of active power losses in the network, due to the reactive power flows in the lines, $Ploss_{reg}$, as a percentage of the active power losses in the base case $Ploss_{unreg}$. In a similar way, a third parameter is defined in this paper:

C)   Inverters Power Losses Index:

$$IL\% = \frac{Pinv_{reg} - Pinv_{unreg}}{Pinv_{unreg}}100 \qquad (11)$$

The *IL* defines the amount of active power losses in all the inverters, due to the different reactive power delivered, Pinvreg, as a percentage of the inverter losses in the base case, Pinvunreg. The results obtained in Section 3 for the scenario 1 are used as the base case. Therefore, the three parameters provide three performance indices, useful for the comparison of the different reactive power control strategies and the different number of storage in the grid. A lower value of these indices represents a better performance (they can also assume negative values). The reactive power based voltage control strategies evaluated in this section are: fixed $\cos\varphi = 0.9$, $\cos\varphi$ (P), Q(U) and a mixed strategy $\cos\varphi$ (P,U). While the first three strategies are described in many grid codes, the last one is proposed in [9]. A dynamic simulation was run for each different control strategy. The issues on the voltage quality are fulfilled in all the simulations, since the voltage is less than 1.1 *p. u.* at all nodes. The trend of *QDI*, *PLI,* and *IL*, in Scenario 1, is plotted in fig. 10. Table 3 shows the effect of the storage for each control strategies.
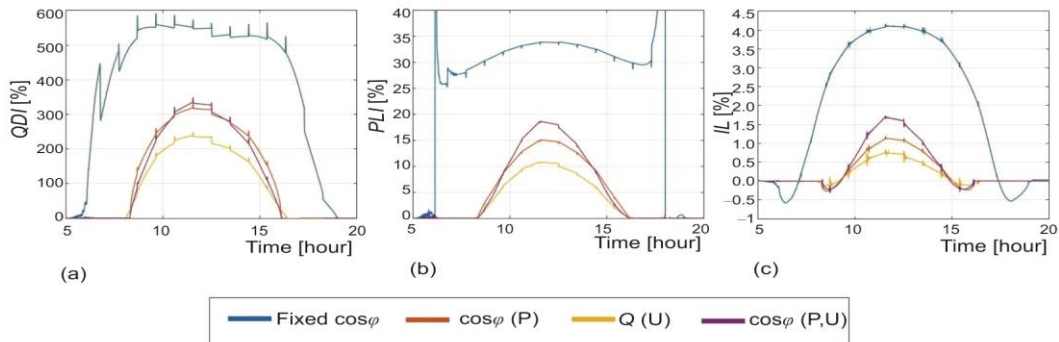

Figure 10. Performance indice; *QDI* (a), *PLI* (b) and *IL* (c) in the base case
(*for color image see journal web site*)

It is noticeable that QDI reaches very high values, since the voltage control strategies under study are based on the reactive power. The worst case is for fixed $\cos\varphi$ method, because of the high amount of reactive energy required from the external grid during the whole regulation. In this case, the PV inverters need to work at the limits of their capability curves all day long. The other strategies require lower values of reactive power, particularly during the starting and the ending parts of the regulation period, therefore they require lower amount of total reactive energy for the regulation.

As expected, a high amount of reactive power flowing into the lines causes an increase of the active power losses due to the increase of the magnitude of the current vector.

S894

Garozzo, D., *et al.*: Comparison of the Reactive Control Strategies in …
THERMAL SCIENCE: Year 2018, Vol. 22, Suppl. 3, pp. S887-S896

Table 3. Daily mean values of *QDI*, *PLI*, and *IL* in the Scenarios 1-4

		Fixed cosφ	cosφ (P)	Q(U)	cosφ (P,U)
Scenario 1	*QDI* [%]	248.05	81.05	57.57	77.02
	PLI [%]	16.55	3.28	2.27	3.60
	IL [%]	1.32	0.16	0.11	0.23
Scenario 2	*QDI* [%]	248.05	78.43	55.13	73.26
	PLI [%]	−202.86	−216.25	−217.20	−216.07
	IL [%]	1.04	−0.09	−0.15	−0.04
Scenario 3	*QDI* [%]	248.78	71.22	50.10	66.14
	PLI [%]	−862.36	−875.11	−875.91	−874.99
	IL [%]	0.14	−0.92	−0.95	−0.88
Scenario 4	*QDI* [%]	250.28	61.49	41.77	53.93
	PLI [%]	−1972.2	−1981.7	−875.9	−1981.8
	IL [%]	−1.36	−2.29	−2.30	−2.28

This behavior is noticeable from the *PLI* curve. It is worth noticing that, at a certain time, the PV output perfectly meets the local demand, reducing the network losses. Therefore, since the value of the denominator is close to zero in eq. (10), the parameter *PLI* diverges in these points. The values of *PLI* in these two points, in fig. 10(b), do not contain meaningful information. Interesting considerations come from the parameter *IL*. For low level of voltage regulation, *IL* reaches negative values. The explanation of this phenomenon could be related to the nature of eq. (1). For low level of regulation, the effect of the control on V_{DC}, *i. e.* the voltage at the DC bus of the inverter, is predominant on the inverter efficiency with respect to the increase of the apparent power delivered. For high level of regulation, the increase of the apparent power has a high impact on the inverter efficiency.

The presence of the storage in the network allows drastically reducing the indices, except for *QDI* in the case of fixed cosφ regulation. This is due to the fact that the BESSs inject active power into the network during their discharge, causing an extra reactive power absorption. The installation of a certain number of BESS reduces the power losses in the network and in the inverters, due to the voltage regulation, with respect to the base case. This condition could represent and advantage for the distribution system operator.

In tab. 4, the energy losses of the different scenarios are exposed, as a percentage of the energy losses calculated in Scenario 1. Network losses, inverter losses and battery losses are taken into account:

$$E_{\text{losses,tot}} = E_{\text{losses,net}} + E_{\text{losses,inv}} + E_{\text{losses,BESS}} \tag{12}$$

Table 4. Percentage of total energy losses with respect to the case with no storage

	Fixed cosφ	cosφ (P)	Q(U)	cosφ (P,U)
Scenario 2	105 %	97 %	97 %	97 %
Scenario 3	99 %	92 %	92 %	91 %
Scenario 4	91 %	83 %	84 %	82 %

It is important to understand the different contribution of the losses in the network, the losses in the converters and the losses in the batteries to the total amount of energy losses.
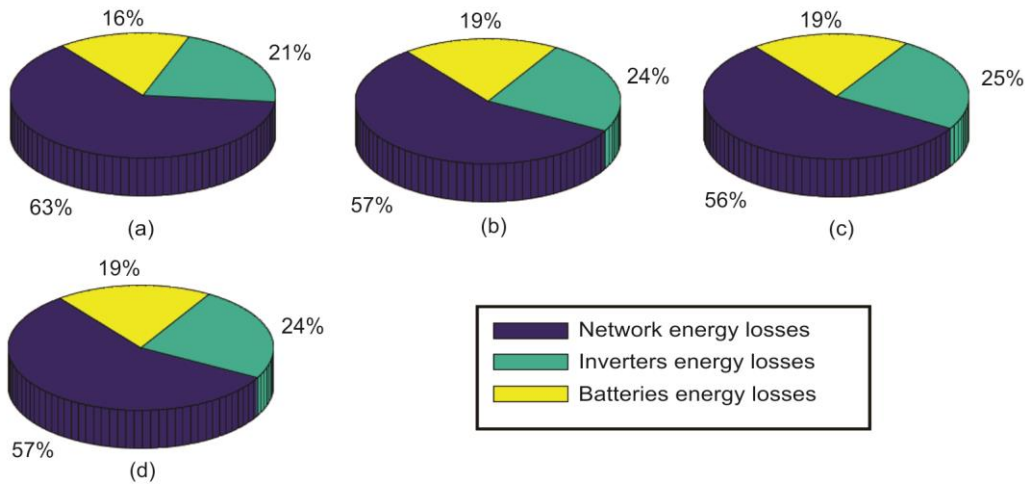
Garozzo, D., *et al.:* Comparison of the Reactive Control Strategies in …
THERMAAL SCIENCE: Year 2018, Vol. 22, Suppl. 3, pp. S887-S896

S895

Figure 11. Different contributions to the total energy losses for the different control strategies in Scenario 4; fixed cosφ (a), cosφ (P) (b), Q(U) (c), fixed cosφ (P,U) (d)

Figure 11 shows the percentages of these contributions in Scenario 4 (9 BESS). In case of fixed cosφ control, the contribution of the network losses to the total energy losses is more relevant than in case of different reactive control strategies, since it reaches the 63% of the total amount of energy losses in the power system. Therefore, this kind of regulation strategy represents the worst case also in terms of thermal energy that must be dissipated in the network, reducing the capacity of the lines.

Conclusion

In this study, the benefits of storage systems combined with reactive power based voltage support strategies for reducing overvoltage in the LVDN due to high PV penetration is investigated. BESS can contribute to the overvoltage prevention by absorbing active power during the peak hours of the PV output. The study shows that combining BESS-s with reactive power based voltage support strategies can decrease the active losses of a distribution network, by the reduction of the reactive power required from the external grid. The aim of this work is to encourage the use of a combined strategy for the voltage control, in which all the distributed resources, as PV systems and storage systems, contribute to the ancillary services. This contribution can support increasing the penetration of renewable energy sources in the LVDN.

Nomenclature

$I_{a,n}$ – component of the current vector at node n on a-axis, [A]

$I_{b,n}$ – component of the current vector at node n on b-axis, [A]

$I_{d,n}$ – component of the current vector at node n on d-axis, [A]

$I_{q,n}$ – component of the current vector at node n on q-axis, [A]

$I_{a,k}$ – component of the current vector at node k on a-axis, [A]

$I_{b,k}$ – component of the current vector at node k on b-axis, [A]

P, Q – active and reactive power

PF – power factor

P_n – active power injected in node n [W]

Q_n – reactive power injected in node n [VAr]

X, R – reactance and resistance ratio

R_k – resistance of line k [Ω]

X_k – reactance of line k [Ω]

$V_{a,n}$ – component of the voltage vector at node n on a-axis, [V]

$V_{b,n}$ – component of the voltage vector at node n on b-axis [V]

$V_{d,n}$ – component of the voltage vector at node n on d-axis [V]

$V_{q,n}$ – component of the voltage vector at node n on q-axis [V]

V_n – Amplitude of the voltage vector at node n [V]

V_{DC} – Voltage at the DC bus of the inverter [V]

V_{AC} – Voltage at the AC bus of the inverter [V]

Greek symbol

θ_n – transformation angle [rad]

Acronyms

P.U. – per unit method

RL – model of a distribution line

References

[1] ***,Trends 2016 in Photovoltaic Application, IEA

[2] ***, GSE, Statistical report – Solar photovoltaic, 2014. (in Italian language).

[3] Arritt, R. F., Dugan, R. C., Distribution System Analysis and the Future Smart Grid, *IEEE Transactions on Industrial Application, 47*, (2011), 6, pp. 2343-2350

[4] Appen, J., *et al*., Time in the Sun, *IEEE Power Energy Mag.*, *11* (2013), 2, pp. 55-64

[5] Bignucolo, F., *et al*. Impact of Distributed Generation Grid Code Requirements on Islanding Detection in LV Networks, *Energies, 10* (2017), 2, pp. 156-171

[6] ***, European Committee for Electrotechnical Standardization, Requirements for Micro-Generating Plants to be Connected in Parallel with Public Low-Voltage Distribution Networks; European Standard CENELEC EN 50438; CENELEC: Brussels, Belgium, 2016

[7] ***, Standard EN 50160, Voltage Characteristics of Electricity Supplied by Public Distribution Networks, Cenelec 2010

[8] Craciun, B. I., *et al*., Frequency Support Functions in Large PV Power Plants with Active Power Reserves, *IEEE Journal of Emerging and Selected Topics in Power Electronics, 2* (2014), 4, pp. 849-858

[9] Demirok, E., *et al*., Local Reactive Power Control Methods for Overvoltage Prevention of Distributed Solar Inverters in Low-Voltage Grids, *IEEE Journal of Photovoltaics, 1* (2011), 2, pp. 174-182

[10] Demirok, E., *et al*., Investigation of Extra Power Loss Sharing Among Photovoltaic Inverters Caused by Reactive Power Management in Distribution Networks, *Proceedings*, IEEE Energy Conversion Congress and Exposition, Pittsburgh,. Penn., USA, 2014

[11] Dall'Anese, E., *et al*., Decentralized Optimal Dispatch of Photovoltaic Inverters in Residential Distribution Systems, *IEEE Trans. Energy Convers.*, *29* (2014), 4, pp. 957-967

[12] Yao, L.W., *et al*., Modeling of Lithium-Ion Battery using MATLAB/Simulink, *Proceedings*, Industrial Electronics Society, IECON 2013-39th Annual Conference of the IEEE, Vienna, 2013

[13] Chen, M., Rincon-Mora, G. A., Accurate Electrical Battery Model Capable of Predicting Runtime and IV performance, *IEEE transaction on energy conversion, 21* (2006), 2, pp. 504-511

[14] Tina, G. Celsa, G., A Matlab/Simulink Model of a Grid Connected Single-Phase Inverter, *Proceedings*, 50th International Universities Power Engineering Conference, Stoke on Trent, UK, 2015

[15] Chivelet, N. M., *et al*., Modeling and Reliability of Inverters for Autonomous Photovoltaic Installations from Measures with Resistive and Reactive Loads (in Spanish)., *Proceedings*, VII Congrese Iberico of Solar Energy, Vigo, Spain, 1994

[16] Gomez, L. D., Modeling for the Simulation, Design and Validation of Photovoltaic Inverters Connected to the Electrical Grid (in Spanish), M. Sc. thesis, Technical School of Industrial Engineering, Madrid, 2011

[17] Braun, M., Reactive Power Supplied by PV Inverters–Cost-Benefit-Analysis, Proceedings, 22nd European Photovoltaic Solar Energy Conference and Exhibition, Milan, Italy, 2007

[18] Cabrera-Tobar, A., *et al*., Capability Curve Analysis of Photovoltaic Generation Systems, *Solar Energy 140* (2016), Dec., pp. 255-264

[19] Pompodakis, E. E., *et al*., Photovoltaic Systems in Low-Voltage Networks and overvoltage Correction with Reactive Power Control, *IET Renewable Power Generation, 10* (2016), 3, pp. 410-417

[20] Ishaq, J., *et al*., Voltage Control Strategies of Low Voltage Distribution Grids Using Photovoltaic Systems, *Proceedings*, Energy Conference (ENERGYCON), 2016 IEEE International. IEEE, Budapest, Hungary, 2016